

This article was downloaded by: [University of Haifa Library]

On: 08 August 2012, At: 14:23

Publisher: Taylor & Francis

Informa Ltd Registered in England and Wales Registered Number: 1072954 Registered office: Mortimer House, 37-41 Mortimer Street, London W1T 3JH, UK



## Molecular Crystals and Liquid Crystals

Publication details, including instructions for authors and subscription information:

<http://www.tandfonline.com/loi/gmcl20>

### A Study of Reentrant Smectic Ordering in Hydrogen Bonded Ferroelectric Dodecyloxy Benzoic Acid and Tartaric Acid Liquid Crystal

V. N. Vijayakumar<sup>a</sup>, K. Murugadass<sup>b</sup> & M. L. N. Madhu Mohan<sup>a</sup>

<sup>a</sup> Liquid Crystal Research Laboratory (LCRL), Bannari Amman Institute of Technology, Sathyamangalam, India

<sup>b</sup> Bannari Amman Vidhya Niketan, Sathyamangalam, India

Version of record first published: 01 Mar 2010

To cite this article: V. N. Vijayakumar, K. Murugadass & M. L. N. Madhu Mohan (2010): A Study of Reentrant Smectic Ordering in Hydrogen Bonded Ferroelectric Dodecyloxy Benzoic Acid and Tartaric Acid Liquid Crystal, *Molecular Crystals and Liquid Crystals*, 517:1, 43-62

To link to this article: <http://dx.doi.org/10.1080/15421400903290675>

PLEASE SCROLL DOWN FOR ARTICLE

Full terms and conditions of use: <http://www.tandfonline.com/page/terms-and-conditions>

This article may be used for research, teaching, and private study purposes. Any substantial or systematic reproduction, redistribution, reselling, loan, sub-licensing, systematic supply, or distribution in any form to anyone is expressly forbidden.

The publisher does not give any warranty express or implied or make any representation that the contents will be complete or accurate or up to date. The accuracy of any instructions, formulae, and drug doses should be independently verified with primary sources. The publisher shall not be liable for any loss, actions, claims, proceedings, demand, or costs or damages whatsoever or howsoever caused arising directly or indirectly in connection with or arising out of the use of this material.

# A Study of Reentrant Smectic Ordering in Hydrogen Bonded Ferroelectric Dodecyloxy Benzoic Acid and Tartaric Acid Liquid Crystal

V. N. VIJAYAKUMAR,<sup>1</sup> K. MURUGADASS,<sup>2</sup> AND  
M. L. N. MADHU MOHAN<sup>1</sup>

<sup>1</sup>Liquid Crystal Research Laboratory (LCRL), Bannari Amman Institute of Technology, Sathyamangalam, India

<sup>2</sup>Bannari Amman Vidhya Niketan, Sathyamangalam, India

*A linear hydrogen bonded homologous liquid crystal series has been isolated with chiral ingredient as levo tartaric acid possessing two chiral carbons and non chiral mesogen as p-n-alkoxy benzoic acids. In the synthesized hydrogen bonded complexes the p-n-alkoxy benzoic acid moiety varied from pentyloxy to dodecyloxy with an exception of butyloxy and hexyloxy benzoic acids. Textural studies have been carried out by polarizing microscopic studies, (POM). Interestingly the phase sequences exhibited by odd and even complexes are strikingly different. In other words phase sequence of Nematic, smectic C\*, F\*, and G\* is observed in the odd hydrogen bonded complexes while in addition to these phases the even counter parts exhibit a new type of phase sequence with smectic C\* followed by pseudo smectic C\* and reentrant smectic C\* phases which are designated as Sm C\*, Sm C\*, and Sm C<sub>p</sub>\* phases respectively. A detailed DSC and dielectric studies confirmed the existence of the reentrant phase. We report a new phase which looks like a long worms and designated it as the pseudo smectic C<sub>p</sub>\*. Theoretical arguments are presented towards the existence of reentrant phenomenon. The magnitude and order of the optical pitch in this phase is almost identical to that of traditional smectic C\* phase. Phase diagram is constructed for the homologous series. Results of tilt angle, dielectric relaxations and dielectric permittivity variations are discussed.*

**Keywords** Levo tartaric acid; p-n-alkoxy benzoic acid; pseudo smectic C<sub>p</sub>\*; re-entrant smectic ordering

## 1. Introduction

The discovery of first ferroelectric liquid crystal by Meyer [1] generated much interest on these soft materials. Recently, hydrogen bonded liquid crystals (HBLC) [2–13], have been designed and synthesized from materials selected on the basis of their molecular reorganization and self-assembly capability. The applicational aspects [14–18] and commercial viabilities made many research groups to work on these soft materials. Hydrogen-bonded liquid crystalline materials are known since early 1960

---

Address correspondence to M. L. N. Madhu Mohan, LCRL, Bannari Amman Institute of Technology, Sathyamangalam 638-401, India. E-mail: mln.madhu@gmail.com

[3,4]; however, recently, [5–13,19–22] much work has been done on these complexes. Hydrogen bond, which is a fifth type of fundamental force, enables various mesogenic and non-mesogenic compounds to form complexes which exhibit rich phase polymorphism. HBLC usually are composed of a proton donor and acceptor molecules. The reported data [5–12,19–22] indicates the fact that if HBLC materials are mesogenic, it is enough either one of proton donor or an acceptor molecule exhibits mesogenic property. The chemical molecular structure [19–22] of HBLC is correlated to the physical properties exhibited by it.

The reported literature suggests the formation of HBLC through carboxylic acids as well as from mixtures of unlike molecules capable of interacting through H-bonding [2,7,10,13–21]. Usually, in all these HBLCs the rigid core is made up of covalent and non-covalent hydrogen bonding. Discovery of HBLC by Kato and Frechet [14] opened a new chapter in synthesis, design, and characterization of these mesogens which facilitated many research groups [26–32] to work in this field.

Cladis [33] reported the first ever reentrant nematic phase sequence in a binary liquid crystal mixture. The reemergence of higher symmetry nematic phase at lower temperatures is considered to be unusual though reentrant phases are reported [34] in ferroelectric systems. In the literature most of the reentrant phase sequence observed in monocomponent systems is with cyano groups [35,36]. Many compounds are reported [36,37] to exhibit double reentrant phase sequence where nematic and smectic A phases are observed to be reentrant. Triple reentrant phenomenon is also reported [38] in a few liquid crystalline systems. The reported literature [39–44] on reentrant phenomenon observed in carboxylic acids as proton donor in the inter hydrogen bonded complexes paved way for various theoretical modeling of liquid crystals.

With our previous experience [24,25,45,46] in designing, synthesizing liquid crystals and in continuation of our efforts to understand hydrogen bonded mesogens in the present work a successful attempt has been made to design and isolate a homologous series of hydrogen bonded ferroelectric liquid crystals (HBFLC) with an aim to study the reentrant smectic ordering. The mesogenic p-n-alkoxybenzoic acids (where n represents the alkoxy carbon number from 5 to 12 except 4 and 6) formed a hydrogen bond with liquid crystal levo tartaric acid respectively. Phase diagrams, mesogenic phase and thermal range are discussed for the decyloxy and dodecyloxy hydrogen bonded benzoic acid complexes which are referred as LTA + 11BA and LTA + 12BA respectively.

## 2. Experimental

Optical textural observations were made with a Nikon polarizing microscope equipped with Nikon digital CCD camera system with 5 mega pixels and 2560 \* 1920 pixel resolutions. The liquid crystalline textures were processed, analyzed and stored with the aid of ACT-2U imaging software system. The temperature control of the liquid crystal cell was equipped by Instec HCS402-STC 200 temperature controller (Instec, USA) to a temperature resolution of  $\pm 0.1^\circ\text{C}$ . This unit is interfaced to computer by IEEE-STC 200 to control and monitored the temperature. The liquid crystal sample is filled by capillary action in its isotropic state into a commercially available (Instec, USA) polyamide buffed cell with 4 micron spacer. Silver wires were drawn as leads from the cell. HP 4192A LF impedance analyzer was used for

dielectric studies. Optical extinction technique was used for determination of tilt angle. The transition temperatures and corresponding enthalpy values were obtained by differential scanning calorimetry (DSC) (Shimadzu DSC-60). Infrared spectroscopy (FTIR) spectra was recorded (ABB FTIR MB3000) and analyzed with the MB3000 software. The 4-undecyloxy benzoic acid and 4-dodecyloxy benzoic acid each with purity of 98% and levo tartaric acid with purity of 99% were supplied by Sigma Aldrich, Germany, and all the solvents used were E.Merk grade.

### 3. Synthesis of HBFLC

Intermolecular hydrogen bonded ferroelectric mesogens are synthesized by the addition of two moles of p-n-alkoxybenzoic acids (nBA) with one mole of levo tartaric acid in N,N-dimethyl formamide (DMF), respectively. Further, they are subject to constant stirring for 12 hours at ambient temperature of 30°C till a white precipitate in a dense solution is formed. The white crystalline crude complexes so obtained by removing excess DMF are then recrystallized with dimethyl sulfoxide (DMSO), and the yield varied from 85% to 95%. Yield of higher homologues complexes are observed to be more compared to its lower counterparts. The molecular structure of the present homologous series of p-n-alkoxy benzoic acids with levo tartaric acid is depicted in the Fig. 1, where n represents the alkoxy carbon number. From the Fig. 1, the alternate hydrogen bonded sites along with two chiral carbons can be identified.

### 4. Results and Discussion

All the mesogens isolated under the present investigation are white crystalline solids and are stable at room temperature. They are insoluble in water and sparingly soluble in common organic solvents such as methanol, ethanol, and benzene and dichloro methane. However they show a high degree of solubility in coordinating solvents like dimethyl sulfoxide (DMSO) and pyridine. All these mesogens melt at specific temperatures below 150°C (Table 1). They show high thermal and chemical stability when subjected to repeated thermal scans performed during POM and DSC studies.

#### 4.1. Infrared Spectroscopy (FTIR)

IR spectra of free p-n-alkoxy benzoic acid, levo tartaric acid and their intermolecular H-bonded ferroelectric complexes were recorded in the solid state (KBr) at room temperature. Figure 2 illustrates the FTIR spectra of the hydrogen bonded complex of LTA + 12BA in solid state at room temperature as a representative case. The solid state spectra of free alkoxybenzoic acid is reported [48] to have two sharp bands at

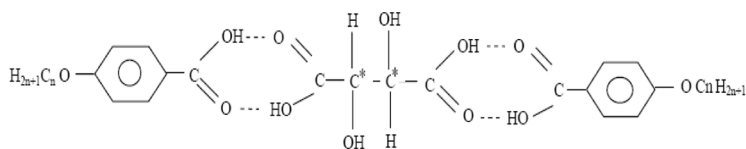


**Figure 1.** Molecular structure of LTA + nBA inter hydrogen bonded complex.

**Table 1.** Comparison of transition temperatures obtained by various techniques

Carbon number	Phase variance	Technique	Crystal Melt	N	C*	C <sub>p</sub> *	C <sub>r</sub> *	F*	G*	Crystal
11	N C* G*	DSC (h)	97.84 (47.68)	140.21 (2.33)	129.37 (2.47)				#	
		DSC (c)		136.78 (2.96)	125.5 (2.12)				84.84 (12.81)	72.54 (8.55)
		POM (c)		137.1	126.2				85.3	72.9
		Dielectric 10 KHz		134.9	128.2				87.3	69.0
		studies (c)		135	128.4				87.3	68.9
12	N C* C <sub>p</sub> * C <sub>r</sub> * F* G*	DSC (h)	97.42 (101.12)	139.11 (1.60)	133.51 (2.12)			125.51 (0.29)	#	
		DSC (c)		141.83 (1.64)	130.78 (0.99)	129.46 (0.31)	127.93 (0.26)	118.83 (0.38)	84.16 (38.06)	63.51 (19.70)
		POM (c)		142.1	131.2	129.2	128.4	119.2	85.8	63.9
		Dielectric 10 KHz		142	132	129.5	127.5	119	84.2	64.1
		studies (c)								

# Monotropic transition.  
(c) cooling run.  
(h) heating run.

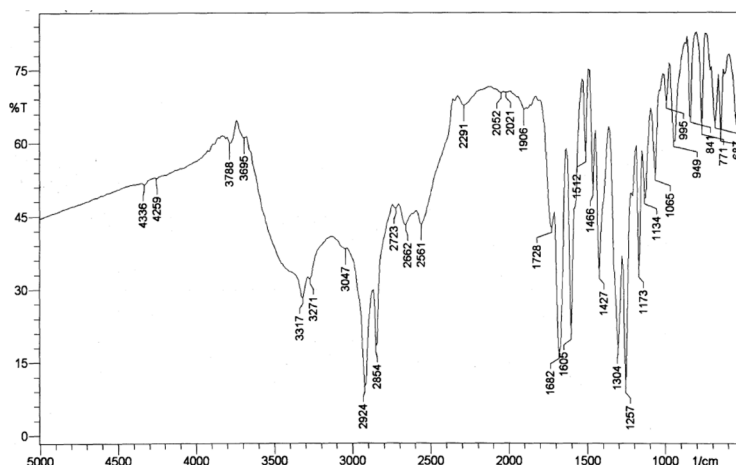


**Figure 2.** FTIR spectra of LTA + 12BA inter hydrogen bonded complex.

$1685\text{ cm}^{-1}$  and  $1695\text{ cm}^{-1}$  due to the frequency  $\nu(\text{C}=\text{O})$  mode. The doubling feature of this stretching mode confirms the dimeric nature of alkoxybenzoic acid at room temperature [20,22]. Further a strong intense band appearing at  $2924\text{ cm}^{-1}$  in Fig. 2 is assigned to  $\nu(\text{O-H})$  mode of the carboxylic acid group.

The doubling nature of  $\nu(\text{C}=\text{O})$  mode may be attributed to the dimeric nature of acid group at room temperature [48]. Corresponding spectrum of solution state (chloroform) show a strong intense band suggesting the existence of monomeric form of benzoic acid. A noteworthy feature in the spectra of LTA + 12BA complex is the appearance of the sharp band at  $1682\text{ cm}^{-1}$  and non-appearance of the doubling nature of  $\nu(\text{C}=\text{O})$  mode of benzoic acid moiety. This clearly suggests that the dimeric nature of the benzoic acid dissociates and prefers to exist in a monomeric form upon complexation.

#### 4.2. Phase Identification

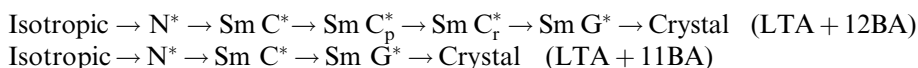
The observed phase variants, transition temperatures, and corresponding enthalpy values obtained by DSC in cooling and heating cycles for the LTA + 11BA and LTA + 12BA complexes are presented in Table 1.

#### 4.3. LTA + *n*BA Homologous Series

A glass slide is rubbed in uni direction for the formation of grooves, and a thin film of sample is sandwiched between a cover slip and the glass substrate. Also the liquid crystalline sample is filled in a commercially available (Instec) polyamide buffered cell of 4 micron thickness. Thus textures are recorded for the liquid crystal sample prepared by above two techniques. This will enable to get a uniformly aligned, well-ordered, and properly oriented sample. The variations in the textures are because of the anchoring energy possessed by the molecules with the glass substrate and different orientations of the molecules. Nematic is the simplest liquid crystalline phase, and it has long range orientational order but lacks positional and bond orientational order. In other words, nematic is imposing the simplest orientational order on a

collective molecules. The anchoring energy for this phase is relatively less compared to any of the smectic phases. Any of the chiral smectic phase has at least two unique directions viz. the director and layer normal. The director maintains the constant angle with respect to the layer normal while describing the helical path as the sample is traversed along the direction normal to the smectic planes. The anchoring energy of the molecules to the substrate in any of the smectic orderings is considerable compared to the Nematic phase. Temperature dependent molecular tilt is the primary order parameter in the smectic phases. In addition to these the sample alignment is dependent on the coating of the substrate, temperature of the sample and the applied field.

The mesogens of the levo tartaric acid and alkoxy benzoic acid ferroelectric homologous series are found to exhibit characteristic textures [47], viz., Nematic (droplets), Smectic  $C^*$  (schlieren texture), pseudo Smectic  $C_p^*$  (worm like texture), re-entrant Smectic  $C_r^*$  (schlieren texture), Smectic  $F^*$  (chequered board texture) and Smectic  $G^*$  (multi colored mosaic texture) respectively. The surface anchoring The general phase sequence of the levo tartaric acid and 4-dodecyloxy benzoic acid and 4-undecyloxy benzoic acid in the cooling run can be shown as:



#### 4.4. DSC

DSC thermograms are obtained in heating and cooling cycle. The sample is heated with a scan rate of  $10^\circ\text{C}/\text{min}$  and held at its isotropic temperature for two minutes so as to attain thermal stability. The cooling run is performed with a scan rate of  $10^\circ\text{C}/\text{min}$ . The respective equilibrium transition temperatures and corresponding enthalpy values of the mesogens of the homologous series are listed separately in Table 1. Smectic  $G^*$  phase of both the hydrogen bonded complexes (LTA + 11BA and LTA + 12BA) is observed to be monotropic transition. Polarizing optical microscopic studies also confirm these DSC results along with the results of monotropic transition.

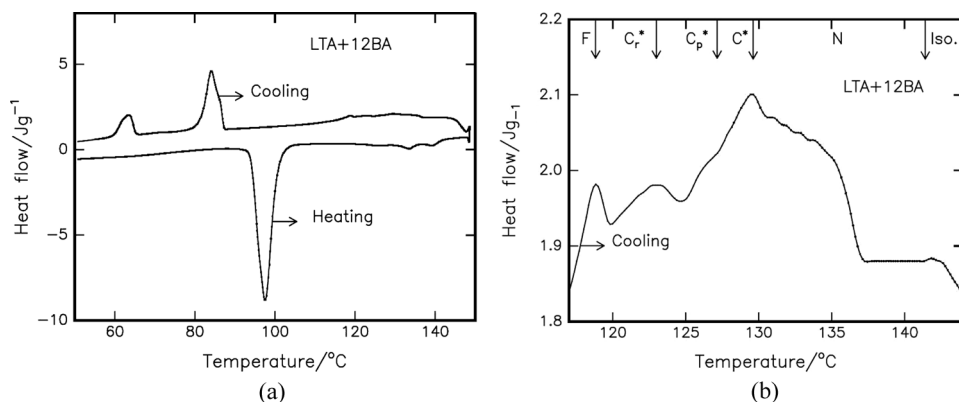


**Figure 3.** (a) DSC thermo gram of LTA + 12BA inter hydrogen bonded complex; (b) DSC thermo gram of LTA + 12BA inter hydrogen bonded complex in the cooling run depicting smectic  $C^*$ ,  $C_p^*$ ,  $C_r^*$  orderings.

#### 4.5. DSC of LTA + 12BA

The phase transition temperatures and enthalpy values of dodecyloxy benzoic acid and levo tartaric acid mesogen (LTA + 12BA) are discussed. From Fig. 3a, b and Table 1, it can be inferred that in the DSC heating run of LTA + 12BA complex, four endothermic peaks are observed at 97.42°C, 139.11°C, 133.51°C, and 125.51°C with enthalpy values of 101.12 m/J, 1.6 m/J, 2.12 m/J, and 0.29 m/J, respectively. These four peaks correspond to crystal-to-melt transition, melt-to-nematic, nematic-to-smectic C\*, and smectic C\*-to-smectic F\*, respectively. It is observed that smectic F\*-to-smectic G\* is monotropic transition in heating. In the cooling run of this sample, seven peaks are observed at 63.51°C, 84.16°C, 118.83°C, 127.93°C, 129.46°C, 130.78°C, and 141.83°C, with enthalpy values of 19.7 m/J, 38.06 m/J, 0.38 m/J, 0.26 m/J, 0.31 m/J, 0.99 m/J, and 1.64 m/J, respectively. These exothermic peaks corresponds to crystal-to-smectic G\*, smectic G\*-to-smectic F\*, smectic F\*-to-smectic C<sub>r</sub>\*, smectic C<sub>r</sub>\*-to-smectic C<sub>p</sub>\*, smectic C<sub>p</sub>\*-to-smectic C\*, smectic C\*-to-Nematic and Nematic to isotropic respectively.

#### 4.6. Phase Diagram of Pure p-n-Alkoxybenzoic Acids

The phase diagrams of pure p-n-alkoxybenzoic acids is reported [23] while the LTA + nBA homologous series is constructed through optical polarizing microscopic studies and by the phase transition temperatures observed in the cooling run of the DSC thermogram. The phase diagram of pure p-n-alkoxybenzoic acid is reported [23] to composed of three phases namely, Nematic, smectic C\* and smectic G\*.

#### 4.7. Phase Diagram of LTA + nBA Homologous Series

The phase diagrams of levo tartaric acid with odd and even p-n-alkoxybenzoic acid complexes are depicted in Figs. 4a and 4b respectively. A careful observation of the Figs. 4a and 4b reveals the following points:

- The mesogenic range has drastically increased from 2°C in LTA + 3BA to 78°C in the last member LTA + 12BA of the homologous series.

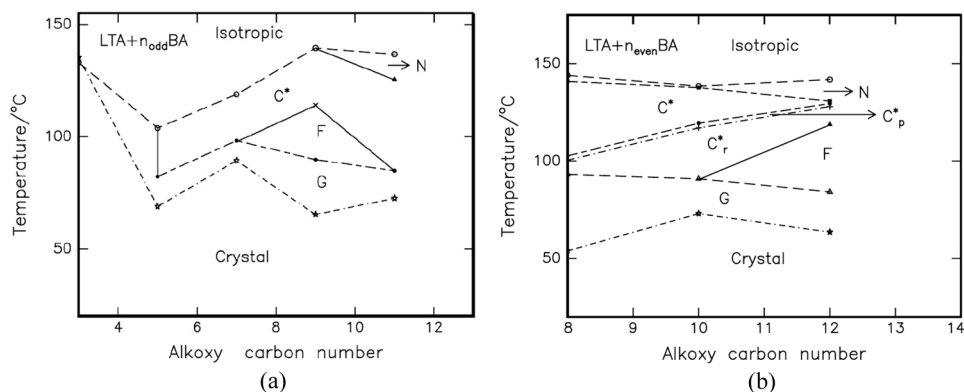


**Figure 4.** (a) Phase diagram of homologous series of LTA + n<sub>odd</sub> BA series; (b) Phase diagram of homologous series of LTA + n<sub>even</sub> BA series.



- b. In addition to the traditional phases like Nematic, smectic  $C^*$ , smectic  $F^*$  and smectic  $G^*$  new phases namely pseudo smectic  $C_p^*$  and re-entrant smectic  $C_r^*$  are observed in the homologous series.
- c. Phase abundance in the odd members of the series with alkoxy carbon numbers 3, 5, 7, 9, and 11 is found to be low compared to its even counter parts.
- d. All the even members of the series with alkoxy carbon numbers 8, 10 and 12 exhibited re-entrant smectic  $C^*$  ordering along with pseudo smectic  $C_p^*$  phase.
- e. Among all the members of the homologous series LTA + 10BA complex has the wide thermal span ( $\sim 26^\circ\text{C}$ ) of reentrant smectic  $C^*$  phase.
- f. Interestingly, the phase sequence of all the members of the homologous series ended with smectic  $G^*$  phase.

## 5. Reentrant Smectic Ordering Phenomenon

LTA + 12BA complex exhibited a reentrant smectic  $C_r^*$  ordering which is evinced through POM, DSC, optical tilt, helical pitch, and dielectric studies which are discussed in the following sections.

### 5.1. POM Studies

As the LTA + 12BA complex is cooled from isotropic, a rich phase abundance is observed as discussed in the previous sections. The phases and corresponding textures observed are the schlieren texture of smectic  $C^*$ , worm-like texture of pseudo-smectic  $C_p^*$ , and schlieren texture of reentrant smectic  $C_r^*$ . These textures are shown in Plates 1 to 4, respectively. Plate 1 depicts the co-existence of schlieren texture of smectic  $C^*$  with worm-like texture of pseudo-smectic  $C_p^*$ . On decreasing the temperature, the fully grown worm-like texture of pseudo-smectic  $C_p^*$  is observed (Plate 2). The transition from pseudo-smectic  $C_p^*$  to reentrant smectic  $C_r^*$  is shown as

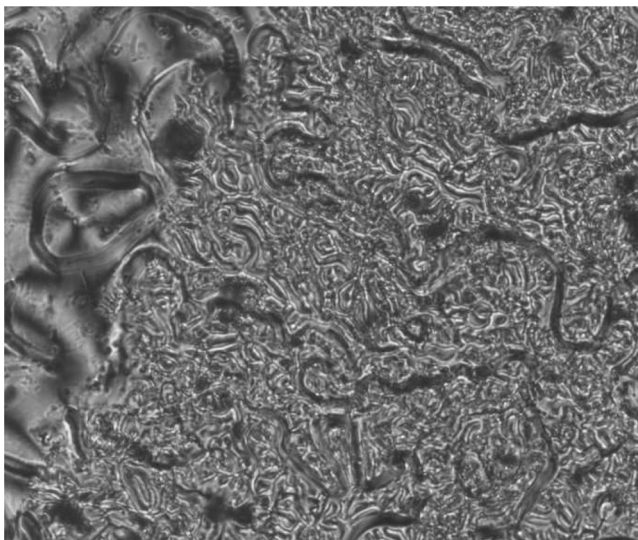


**Plate 1.** Transition from schlieren texture of smectic  $C^*$  to worm-like texture of pseudo smectic  $C_p^*$ .

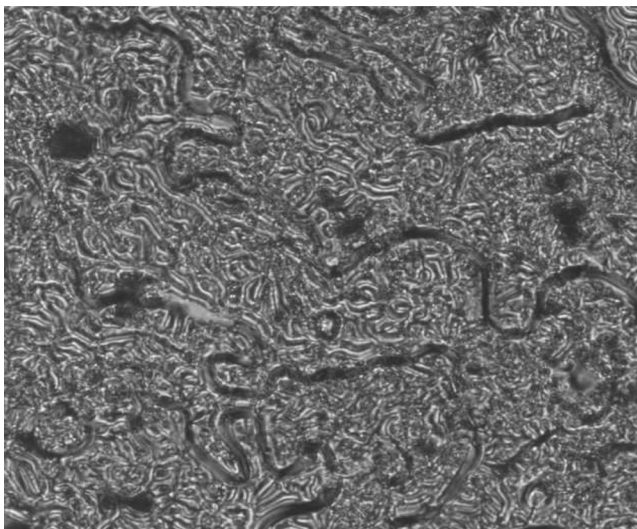


**Plate 2.** Fully grown worm-like texture of pseudo-smectic  $C^*$ .

Plate 3. On further decrease of temperature, stabilization of the reentrant smectic  $C_r^*$  is observed as shown in Plate 4. This optical observation gives the vital textural evidence for pseudo-smectic and reentrant smectic phases designated as  $C_p^*$  and  $C_r^*$ , respectively.

### 5.2. DSC Studies

From the DSC thermogram (Figs. 3a and 3b) of LTA + 12BA the phase transition temperatures of all the phases with particular reference to pseudo smectic  $C_p^*$  and

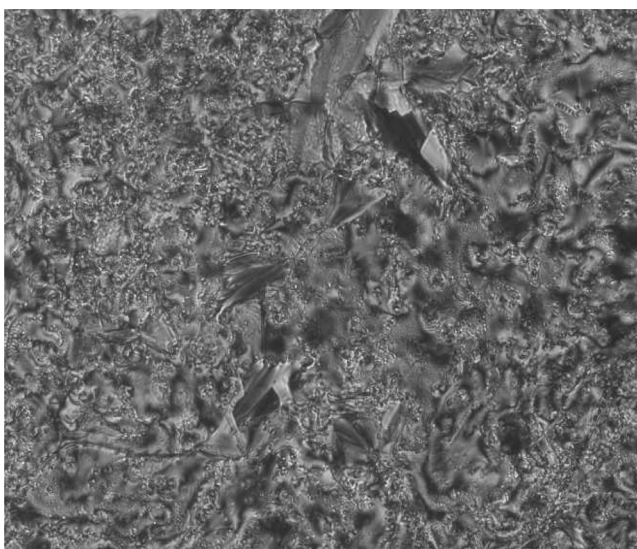


**Plate 3.** Co-existence of pseudo-smectic  $C_p^*$  and reentrant smectic  $C_r^*$ .

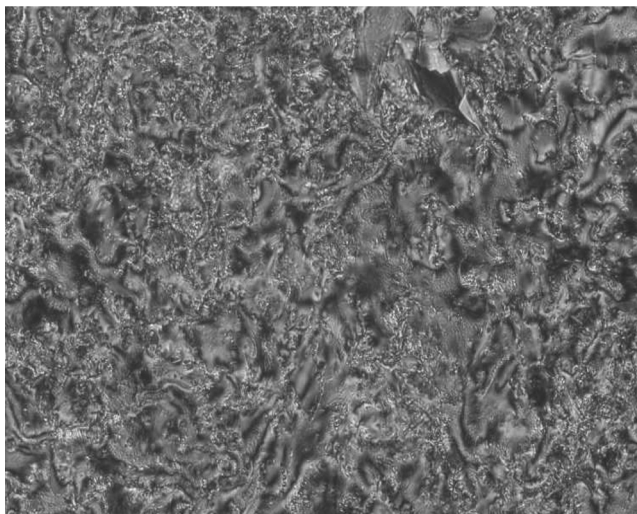


**Plate 4.** Texture of reentrant smectic  $C_R^*$ .

reentrant smectic  $C_r^*$  are detected. This serves as yet another evidence to identify the reentrant phenomenon.

### 5.3. Optical Tilt Angle Studies

Optical tilt angle has been experimentally measured by optical extinction method [49] in the smectic  $C^*$  of LTA + 11BA and LTA + 12BA hydrogen bonded complexes which are depicted in Figs. 5, 6 respectively, while reentrant smectic  $C_r^*$  phase of LTA + 12BA in Fig. 7 respectively. Optical tilt angle in the pseudo smectic  $C_p^*$  phase

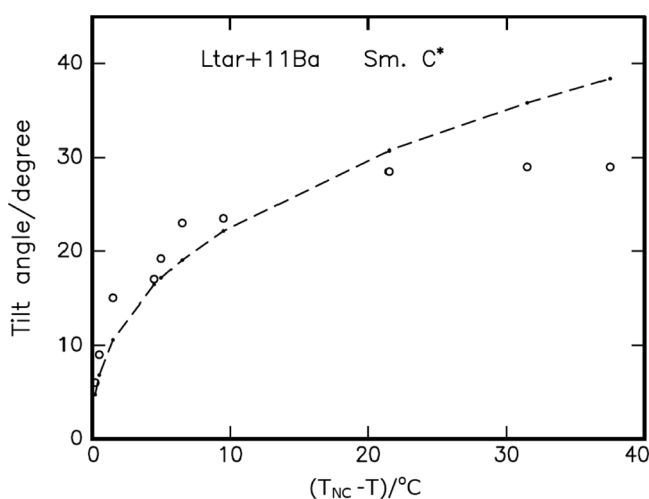


**Figure 5.** Temperature variation of tilt angle in smectic  $C^*$  phase of LTA + 11BA. Solid line denotes the fit.

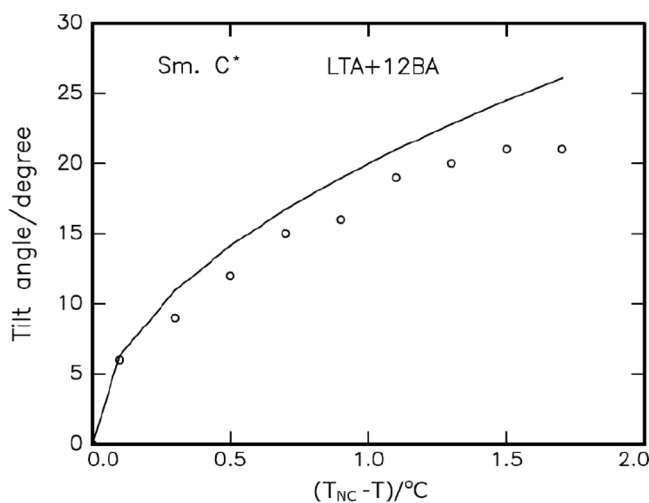


**Figure 6.** Temperature variation of tilt angle in smectic  $C^*$  phase of LTA + 12BA. Solid line denotes the fit.

of LTA + 12BA is illustrated in Fig. 8. In all the above figures the theoretical fit obtained from the mean field theory is denoted by a solid line. From the Figs. 5 and 6, it is observed that the tilt angle increases with decreasing temperature and attains a saturation value. It is interesting to note that the magnitude of tilt angle in re-entrant smectic  $C_r^*$  phase is high compared to its value in smectic  $C^*$ . These large magnitudes of the tilt angle are attributed [31] to the direction of the soft covalent hydrogen bond interaction which spreads along molecular long axis with finite inclination.

Figure 5 illustrates the temperature variation of tilt angle pertaining to smectic  $C^*$  phase of LTA + 11BA complex. It can be noted that tilt angle increases with

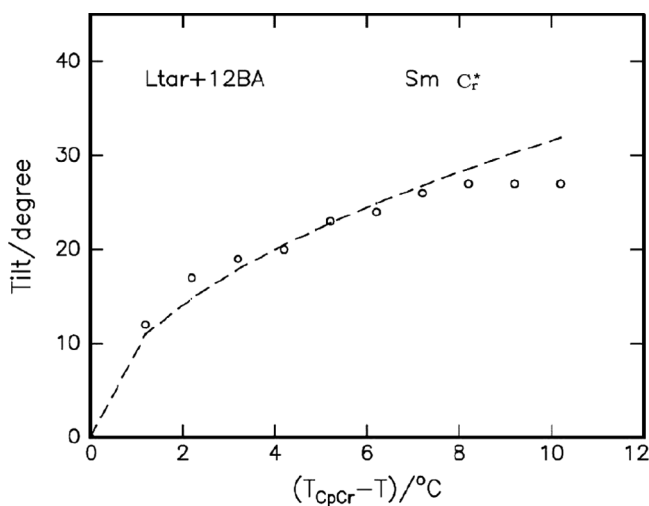


**Figure 7.** Temperature variation of tilt angle in reentrant smectic  $C_r^*$  phase of LTA + 12BA. Solid line denotes the fit.

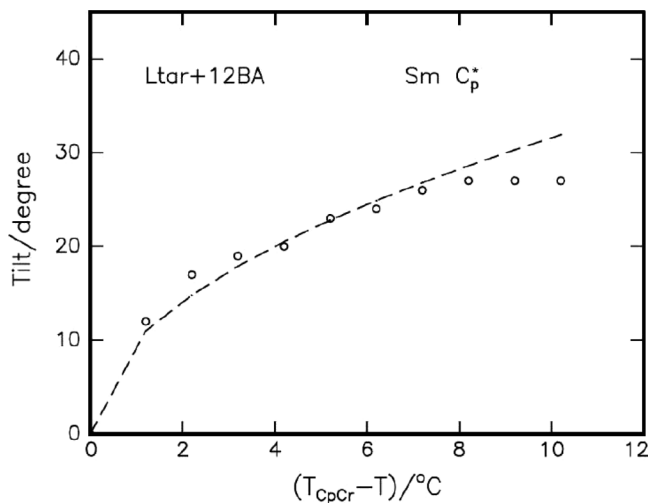


**Figure 8.** Temperature variation of tilt angle in pseudo smectic  $C_p^*$  phase of LTA + 12BA. Solid line denotes the fit.

decreasing temperature and attains a saturated value of  $28^\circ$  at the culmination of the smectic  $C^*$  phase.

Tilt angle is a primary order parameter [18] in ferroelectric phases, viz. smectic  $C^*$  and smectic  $C_r^*$ . The temperature variation is estimated by fitting the observed data of  $\theta(T)$  to the relation

$$\theta(T) \propto (T_{N^*C^*} - T_{C^*})^\beta. \quad (1)$$

The critical exponent  $\beta$  value estimated by fitting the data of  $\theta(T)$  to the above Eq. (1) is found to be 0.50 to agree with the Mean Field [50] prediction. The dotted line in Figs. 5–7 depicts the fitted data. Further, the agreement of  $\beta$  with Mean Field value infers the long-range interaction of transverse dipole moment for the stabilization of tilted smectic  $C^*$  and reentrant smectic  $C_r^*$  phases.

#### 5.4. Dielectric Studies

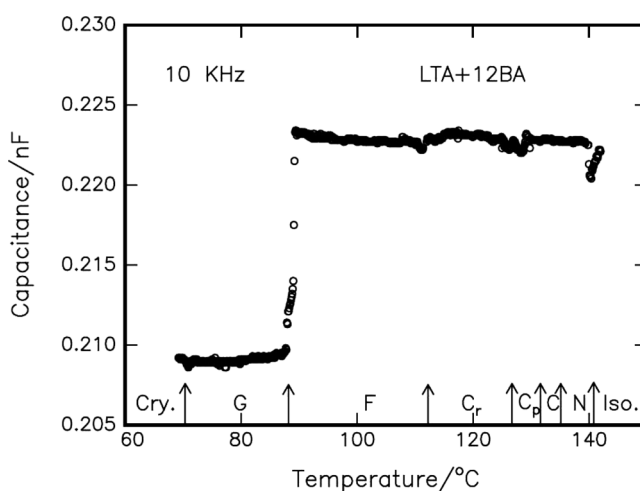
The compound is filled in a commercially available polyamide buffed cell (Instec) of 4 micron spacer with an active area of  $1 \text{ mm}^2$  under capillary action. Silver wires are drawn from the cell as leads. Empty cell is calibrated with temperature and with a known substance (benzene) to calculate the leads capacitance. The cell with the sample is placed in an Instec hot stage (HCS 402) whose temperature is monitored by an Instec stand alone temperature controller (STC 200), interfaced with a computer, to an accuracy of  $\pm 0.1^\circ\text{C}$ . The sample is taken to its isotropic state and held for two minutes so as to attain thermal stability. Simultaneous textural observations are made to ascertain the phase of the mesogen. The readings are noted in the cooling run with a scan rate of  $0.1^\circ\text{C}/\text{min}$ . The LTA + 12BA compound in the cell is provided with a sinusoidal stimulus of 1.1 volts obtained from HP 4192A impedance analyzer. The variation of the capacitance at a frequency of 10 KHz is plotted in

Fig. 9 in which all the phases transition temperatures are observed. Further, reentrant phenomenon is also established by detailed dielectric studies.

From Fig. 9, it is noted that at around  $142^{\circ}\text{C}$  a peak is observed which is attributed to the isotropic to nematic transition. In the entire thermal span of nematic phase the unaltered linear variation of capacitance is observed relating to the stabilization of the phase. A kink is recorded at around  $132^{\circ}\text{C}$  indicating the phase transition from nematic to smectic  $\text{C}^*$  phase. The magnitude of the capacitance suddenly decreased at  $129.5^{\circ}\text{C}$  indicating transition from smectic  $\text{C}^*$  phase to smectic  $\text{C}_p^*$  phase. A small distinguishable peak at  $127.5^{\circ}\text{C}$  in the dielectric spectrum relates to the onset of pseudo smectic  $\text{C}_r^*$  phase transition. The temperature variation of the magnitude of the capacitance in this phase is almost invariant. A small dip at  $119^{\circ}\text{C}$  indicates the onset of smectic  $\text{F}^*$  phase. The stabilization of smectic  $\text{F}^*$  phase in its entire thermal span is seen in the form of unaltered magnitude of the capacitance. A sudden drastic decrement in the magnitude of the capacitance at  $84.2^{\circ}\text{C}$  indicates the onset of smectic  $\text{G}^*$ . The crystallization is observed at  $64.1^{\circ}\text{C}$ . Similar variations are observed in the dielectric loss spectrum of this complex. Figure 10 illustrates the dielectric spectrum of LTA+11BA mesogen at 10 KHz and 100 KHz respectively. All the phase transitions namely, isotropic to nematic, nematic to smectic  $\text{C}^*$ , smectic  $\text{C}^*$  phase to smectic  $\text{G}^*$  phase and smectic  $\text{G}^*$  to crystal are observed. Similar anomalies are observed in dielectric loss spectrum of the corresponding compound.

### 5.5. Origin of Reentrant Phenomenon

The reentrant phenomenon, experimentally discovered [33,37], is attributed to ordering and disordering phase sequence. Further macroscopic theories [39,51] are developed for reproducing reentrant phenomenon. Dipolar frustrations of the molecules play a vital role in inducing the reentrant phenomenon. These dipolar interactions, under the molecular closed packing conditions of these liquid crystals, are responsible for the reentrant phases [44]. Further the interaction between the coupled degrees of



**Figure 9.** Temperature variation of capacitance for LTA + 12BA complex.

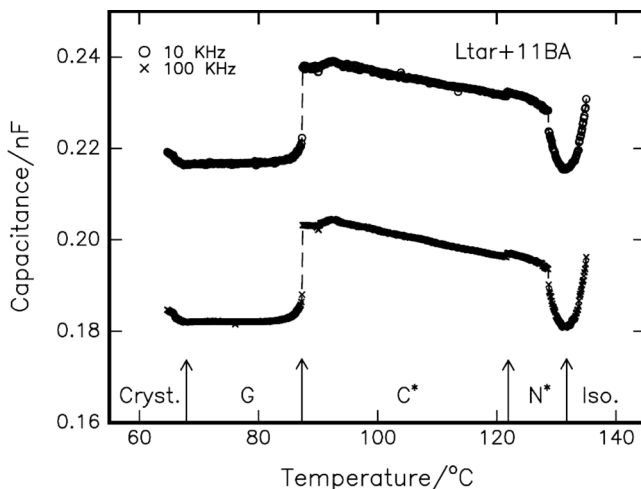


**Figure 10.** Temperature variation of capacitance for LTA + 11BA complex.

freedom of dipolar orientation and molecular positions favor an order–disorder phase sequence. Smectic phases are realized when in the plane normal to the average molecular axis, frustration is lifted by positional fluctuations normal to the plane. These molecular positional fluctuations are referred as permeation fluctuations [52].

Reentrant phase sequence in carboxylic acid are reported [13] in literature. In all these cases, a close observation reveals that the monomerization of the dimers play a vital role in the occurrence of this unusual phase sequence. Cladis [33,34] propose two factors, namely, the layer spacing and packing density, create favorable conditions for the occurrence of reentrant phase sequence. In particular, to liquid crystal mesogens possessing carboxylic acid, in addition to the above two factors, monomerization of the dimers also pave way for reentrant phenomenon.

The rod-like molecules are arranged in smectic layers, and this layer spacing is close to the molecular length. If the length of the molecule is less than the layer spacing the reentrant phenomenon is prevalent. The packing of the monomers is efficient at low temperature. But as the temperature is increased, the density of the medium increases, thereby packing is no longer efficient. The molecules slip of the layers leading to reentrant phases.

## 6. Dielectric Relaxations in Smectic C\* C<sub>r</sub>\* and G\* Phases

Dielectric dispersion i.e., frequency variation of dielectric loss exhibited by LTA + 11BA and LTA + 12BA is studied at different temperatures in smectic C\* and C<sub>r</sub>\* phases in the frequency range of 5 Hz to 13 MHz. An impedance analyzer (HP4192A) is operated with 1V<sub>P-P</sub> oscillating signal with zero bias fields. Relative permittivity  $\epsilon'(\omega)$  and dielectric loss  $\epsilon''(\omega)$  are calculated by the following equations;

$$^*\epsilon'(\omega) = \epsilon'(\omega) - j\epsilon''(\omega) \quad \epsilon'(\omega) = [\text{CLC} - C_{\text{leads}}] / [C_{\text{empty}} - C_{\text{leads}}] \quad ^*\epsilon''(\omega) = \text{Tan}\delta(\omega) \quad ^*\epsilon_r(\omega)$$

To detect the possible relaxation in both the HBFLC complexes, the mesogens are scanned in the frequency range of 5 Hz to 13 MHz at different temperatures

corresponding to various smectic phases. Two types of relaxation mechanisms namely Goldstone Mode (GM) and Type I relaxation are observed in the phases of LTA + 11BA and LTA + 12BA mesogens.

### 6.1. Goldstone Mode

Helix is formed in the smectic layers of the ferroelectric phase. This helix can be unwound by applying suitable field. In the present study, the HBFLC is filled in a  $4\mu$  conducting cell, and suitable voltage is drawn from Impedance analyzer 4192A to study the Goldstone mode.

Goldstone mode is detected in smectic  $C^*$  phase of LTA + 11BA and in smectic  $C_r^*$  phase of LTA + 12BA mesogens, respectively. As reported in other HBFLC [19], Goldstone mode is observed at lower frequencies ( $\sim 5$  KHz) in smectic  $C^*$  and smectic  $C_r^*$  phases of the hydrogen bonded compounds of the present homologous series. The relaxation frequency at  $\sim 5$  KHz in smectic  $C^*$  and smectic  $C_r^*$  phases of LTA + 11BA and LTA + 12BA hydrogen bonded complexes, respectively, are interpreted as due to collective response originated due to the excitation of the coupled transverse dipole moment situated around the chiral centers over the layers in the form of polarization helix. The influence of applied bias on the Goldstone mode relaxation in smectic  $C^*$  of LTA + 11BA and in smectic  $C_r^*$  phases of LTA + 12BA are studied. Further, it is observed that these relaxation are suppressed under different applied fields. This experimental evidence conforms that Goldstone mode is originated from the helix spread over the smectic layers of respective phases. The Arrhenius plots corresponding to the Goldstone mode in smectic  $C_r^*$  phase of LTA + 12BA is depicted in Fig. 11.

### 6.2. Type I Relaxation

In addition to the above discussed Goldstone mode, another type of relaxation, named type I relaxation, is observed in both the mesogens at higher frequencies at

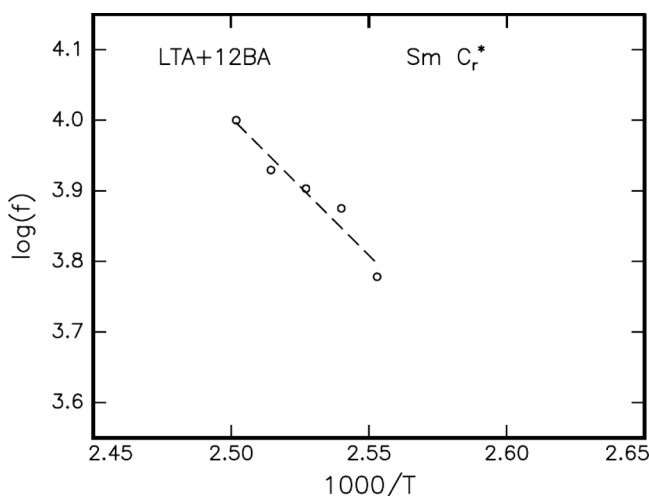


**Figure 11.** Arrhenius plots of LTA + 12BA complex in smectic  $C_r^*$  phase pertaining Goldstone modes.



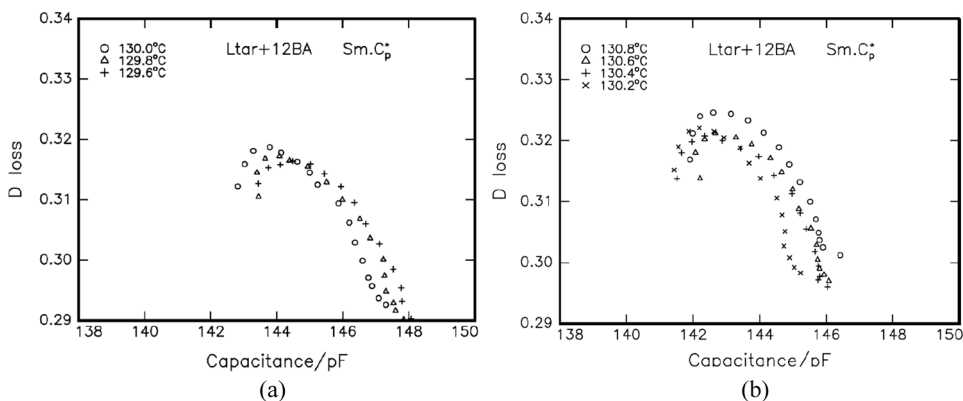


**Figure 12.** (a, b) Cole-Cole plots indicating type I relaxation in pseudo smectic  $C_p^*$  phase of LTA + 12BA.

several mega hertz. In this type of relaxation mechanism, relaxation is not suppressed by the applied field. The type I relaxations are related to the reorientation mechanism of longitudinal dipole moment to the applied field. Further, the reorientation of the longitudinal dipole moment pertaining to the flexible end chain bridged by electronegative oxygen atom is observed to respond rather slowly to the external field in type I relaxation.

In LTA + 12BA complex type I relaxation is detected in smectic  $C_p^*$  phase, smectic  $C_r^*$  phase and smectic  $G^*$  phase at 4.6 MHz, 4.55 MHz, and 4.5 MHz respectively. The Arrhenius shift with respect to temperature is calculated for each individual phase. Figures 12a and 12b depicts the Cole-Cole plots of smectic  $C_p^*$  phase pertaining to LTA + 12BA mesogens at various temperatures. Figure 13 illustrates the Cole-Cole plot in smectic  $G^*$  phase of LTA + 11BA hydrogen bonded complex.

The activation energies of type I for all the phases of both the hydrogen bonded complexes discussed above, are tabulated in Table 2.

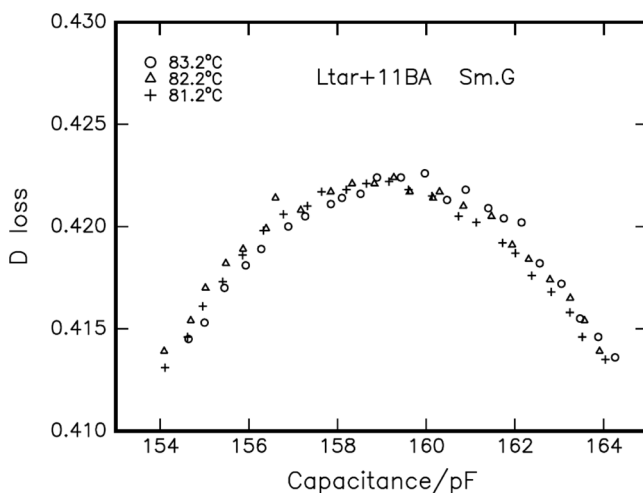


**Figure 13.** Cole-Cole plots indicating type I relaxation in smectic  $G^*$  phase of LTA + 11BA.

**Table 2.** Activation energies and relaxation frequency obtained in various phases of HBFLC complexes

HBFLC	Phase	Relaxation		Activation energy(eV)
		Type	Frequency	
LTA + 12BA	C <sub>p</sub> <sup>*</sup>	Type I	4.60 MHz	0.38
	C <sub>r</sub> <sup>*</sup>		4.55 MHz	0.39
	G <sup>*</sup>		4.50 MHz	0.41
LTA + 11BA	N	Type I	8.40 MHz	0.32
	C <sup>*</sup>		3.57 MHz	0.39
	G <sup>*</sup>		3.30 MHz	0.52

7. Helical Pitch

The pitch of FLC materials is typically in the order of 1–100 μm [55], whereas the thickness of one layer is of the order 20–30 Å. In order to have bistable switching, the helicoidal structure has to be unwound. The most common way of doing this is to sandwich the FLC material between two conducting glass plates in such a way that layer are perpendicular to these structures. The helical pitch is measured by diffraction of He-Ne red laser light on sample, filled in a commercial cell. This method can be used for measurement of the helical pitch of limited length. For pitch shorter than 0.8 μm the diffraction ring is diffused or completely disappears.

Plate 5 illustrates the first and second order diffraction pattern of the helical pitch at 125°C corresponding to smectic C<sub>r</sub><sup>\*</sup> phase of LTA + 12BA complex. The magnitude

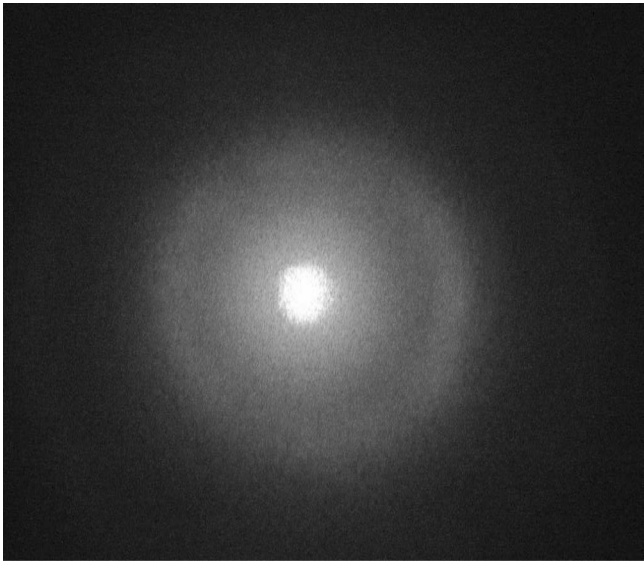


**Plate 5.** Diffraction pattern of helical pitch at 125°C corresponding to smectic C<sub>r</sub><sup>\*</sup> phase of LTA + 12BA complex.

of the helical pitch in smectic  $C_r^*$  phase is found to be  $45\text{ }\mu\text{m}$ . In the smectic  $C^*$  phase of LTA + 11BA and LTA + 12BA complexes, the magnitude of the pitch is found to be  $39\text{ }\mu\text{m}$  at  $120^\circ\text{C}$  and  $40\text{ }\mu\text{m}$  at  $130^\circ\text{C}$ , respectively. Thus from these studies it can be concluded that in LTA + 12BA complex the reentrant phase is smectic ordering.

## Conclusions

An alternate linear hydrogen bonded ferroelectric liquid crystal homologous series has been synthesized. From the transitions temperatures phase diagram is constructed. Reentrant smectic ordering is observed in dodecyloxy benzoic acid and tartaric acid hydrogen bonded complex of the homologous and is characterized by POM, DSC, dielectric, and pitch measurements. Goldstone mode in reentrant smectic  $C_r^*$  phase also indicates that the reentrant phase is smectic ordering.

## Acknowledgements

One of the authors (M. L. N. M. M.) acknowledges the financial support rendered by All India Council for Technical Education, Department of Science and Technology, and Defence Research Development Organization, New Delhi. Infrastructural support provided by Bannari Amman Institute of Technology is gratefully acknowledged.

## References

- [1] Meyer, R. B., Liebert, L., Strezelecki, L., & Keller, P. (1975). *J. Physique. Lett.*, **36**, 69.
- [2] Clark, N. A., & Lagerwall, S. T. (1980). *Appl. Phys. Lett.*, **36**, 899.
- [3] Andersson, G., Dhal, I., Kellr, P., Kuczynski, W., Lagerwall, S. T., Skarp, K., & Stebler, B. (1987). *Appl. Phys. Lett.*, **51**, 640.
- [4] Gouda, F., Skarp, K., & Lagerwall, S. T. (1991). *Ferroelectrics*, **113**, 165.
- [5] Andersson, G., Dhal, I., Kuczynski, W., Lagerwall, S. T., Skarp, K., & Stebler, B. (1988). *Ferroelectrics*, **84**, 285.
- [6] Wang, J. M., Kim, Y. J., Kim, C. J., & Kim, K. S. (2002). *Ferroelectrics*, **277**, 185.
- [7] Aira, H., Ray, H., & Kohki, T. (2004). *Jpn. J. Appl. Phys.*, **43**, 6243.
- [8] Wu, S. L., & Lin, C. Y. (2003). *Liq. Cryst.*, **30**, 205.
- [9] Kumar, P. A., & Pisipati, V. G. K. M. (2000). *Adv. Mater.*, **2**, 1617.
- [10] Kittel, C. (1974). *Introduction to Solid State Physics*, Wiley Eastern Private Limited: New Delhi.
- [11] Luckhurst, G. R., & Gray, G. W. (1979). *The Molecular Physics of Liquid Crystal*, Academic Press: New York.
- [12] (a) Niori, T., Sekine, T., Watanabe, J., Furukawa, J., Choi, S. W., & Takezoe, H. (1996, 1997). *J. Mater. Chem.*, **6**, 1231; (b) *ibid* **7**, 1307.
- [13] (a) Adams, H., Brailly, N., Bruce, D. W., Dhillon, R., Dunmur, D. A., Hunt, S. E., Lalinde, E., Maggs, A. A., Orr, R., Styring, P., Wragg, M. S., & Maitlies, P. M. (1988). *Polyhedron*, **7**, 1861; (b) Mikhaleva, M. A., Kolesnichenko, G. A., Rubina, K. I., Goldberg, Yu. Sh., Savelev, V. A., Leitis, L. Ya., Shimanskaya, M. V., & Mamaev, V. P. (1986). *Chem. Hetro. Compd.*, **22**, 310.
- [14] (a) Kato, T., & Frechet, J. M. J. (1989). *J. Am. Chem. Soc.*, **111**, 8533; (b) Kato, T. (2000). *Hydrogen Bonded Liquid Crystals: Molecular Self-Assembly for Dynamically Functional Materials*, Springer: Heidelberg.

- [15] (a) Kihara, H., Kato, T., Uryu, T., Ujiie, S., Kumar, U., Frechet, J. M. J., Bruce, D. W., & Price, J. D. (1996). *Liq. Cryst.*, 21, 25; (b) Parra, M., & Hidalgo, P. (2005). *J. Alderete, Liq. Cryst.*, 32, 449.
- [16] (a) Brand, H. R., Cladis, P. E., & Pleiner, H. (1992). *Macro. Mol.*, 25, 7223; (b) Cook, A. G., Baumeister, U., & Tschierske, C. (2005). *J. Mater. Chem.*, 15, 1708.
- [17] Goodby, J. W., Blinc, R., Clark, N. A., Lagerwall, S. T., Osipov, S. A., Pikin, S. A., Sakurai, T., Yoshino, Y., & Zecks, B. (1991). *Ferro Electric Liquid Crystal, Principles, Properties, and Applications*, Gordon and Breach Press: Philadelphia.
- [18] de Gennes, P. G. (1974). *The Physics of Liquid Crystals*, Oxford Press: London.
- [19] Sreedevi, B., Chalapathi, P. V., Srinivasulu, M., Pisipati, V. G. K. M., & Potukuchi, D. M. (2004). *Liq. Cryst.*, 31, 303.
- [20] Swathi, P., Kumar, P. A., Pisipati, V. G. K. M., Rajeswari, A. V., Sreehari Sastry S., & Narayana Murty, P. (2002). *Z. Natur. Forsch.*, 57a, 797.
- [21] Noot, C., Perkins, S. P., & Coles, H. J. (2000). *Ferroelectrics*, 244, 331.
- [22] Swathi, P., Kumar, P. A., & Pisipati, V. G. K. M. (2001). *Z. Natur. Forsch.*, 56a, 691.
- [23] Vijayakumar, V. N., Murugadass, K., & Madhu Mohan, M. L. N. (2009). *Mol. Cryst. Liq. Cryst.*, 515, 37.
- [24] Madhu Mohan, M. L. N., Arunachalam, B., & Arravindh Sankar, C. (2008). *Metal and Mater. Trans. A*, 39, 1192.
- [25] Madhu Mohan, M. L. N., & Arunachalam, B. (2008). *Z. Natur. Forsch.*, 63a, 435.
- [26] (a) Madhu Mohan, M. L. N., & Pisipati, V. G. K. M. (2000). *Liq. Cryst.*, 26, 1609; (b) Murugadass, K., Vijayakumar, V. N., & Madhu Mohan, M. L. N. (2010). *Mol. Cryst. Liq. Cryst.*, 517, 41.
- [27] Letellier, P., Ewing, D. E., Goodby, J. W., Haley, J., Kelly, S. M., & Mackenzie, G. (1997). *Liq. Cryst.*, 22, 609.
- [28] Kumar, P. A., Srinivasulu, M., & Pisipati, V. G. K. M. (1999). *Liq. Cryst.*, 26, 1339.
- [29] Rudquist, P., Korblova, E., Walba, D. M., Shao, R., Clark, N. A., & MacLennan, J. E. (1999). *Liq. Cryst.*, 26, 1555.
- [30] Srinivasulu, M., Satyanarayana, P. V. V., Kumarand, P. A., Pisipati, V. G. K. M. (2001). *Liq. Cryst.*, 28, 132.
- [31] Barmatov, E. B., Bobrovsky, A., Barmatova, M. V., & Shibaev, V. P. (1999). *Liq. Cryst.*, 26, 581.
- [32] Sideratou, Z., Tsiourvas, D., Paleos, C. M., & Skoulios, A. (1997). *Liq. Cryst.*, 22, 51.
- [33] Cladis, P. E. (1975). *Phys. Rev. Lett.*, 35, 48.
- [34] Cladis, P. E. (1988). *Mol. Cryst. Liq. Cryst.*, 165, 85.
- [35] Madhusudana, N. V., Sadashiva, B. K., & Moodithaya, K. P. L. (1979). *Curr. Sci.*, 48, 613.
- [36] Hardouin, F., Sigaud, G., Achard, M. F., & Gasparoux, H. (1979). *Solid State Commun.*, 30, 265.
- [37] Hardouin, F., & Levelut, A. M. (1980). *J. de Physique*, 41, 41.
- [38] Nguyen, H. T., Hardouin, F., & Destrade, C. (1982). *J. de Physique*, 43, 1127.
- [39] Berker, A. N., & Waker, J. S. (1981). *Phys. Rev. Lett.*, 47, 1469.
- [40] Indekeu, J. O., & Berker, A. N. (1986). *Rev. Lett.*, 33, 1158.
- [41] Indekeu, J. O., & Berker, A. N. (1986). *Physica (Utrecht)*, 140A, 368.
- [42] Berker, A. N., & Indekeu, J. O. (1987). In: *Incommensurability in Crystals, Liquid Crystals and Quasi-Crystals*, Scott, J. S. (Ed.), Plenum: New York.
- [43] (a) Dowell, F. (1983). *Phys. Rev. A*, 28, 3526; (b) Dowell, F. (1985). *Phys. Rev. A*, 31, 2464; (c) Dowell, F. (1985). *Phys. Rev. A*, 31, 3214.
- [44] Indekeu, J. O., Berker, A. N., Chiang, C., & Garland, C. W. (1987). *Phys. Rev. A*, 35, 1371.
- [45] Pisipati, V. G. K. M., Kumar, P. A., & Madhu Mohan, M. L. N. (2000). *Mol. Cryst. Liq. Cryst.*, 350, 141.
- [46] Madhu Mohan, M. L. N., Kumar, P. A., & Pisipati, V. G. K. M. (2001). *Mol. Cryst. Liq. Cryst.*, 366, 431.

- [47] Gray, G. W., & Goodby, J. W. G. (1984). *Smectic Liquid Crystals: Textures and Structures*, Leonard Hill: London.
- [48] Nakamoto, K. (1978). *Infrared and Raman Spectra of Inorganic and Co-ordination Compounds*, Interscience: New York.
- [49] Patel, J. S., & Goodby, J. W. (1987). *Mol. Crys. Liq. Cryst.*, 144, 117.
- [50] Stanley, H. E. (1971). In: *Introduction to Phase Transition and Critical Phenomena*, Oxford University Press, USA.
- [51] Indekeu, J. O., & Berker, A. N. (1986). *Phys. Rev. A.*, 33, 1158.
- [52] Ocko, B. M., Pershan, P. S., Safinya, C. R., & Chiang, L. Y. (1987). *Phys. Rev. A.*, 35, 1868.
- [53] Cladis, P. E. (1988). *Mol. Crys. Liq. Cryst.*, 165, 85.
- [54] Godua, F., Skarp, K., & Lagerwall, S. T. (1991). *Ferroelectrics*, 113, 161.
- [55] Karapinar, R. (2000). *Turk. J. Phys.*, 24, 115.